THE OFFICIAL MAGAZINE OF THE OCEANOGRAPHY SOCIETY

Oceanography

CITATION

Takahashi, T., C. Sweeney, B. Hales, D.W. Chipman, T. Newberger, J.G. Goddard, R.A. Iannuzzi, and S.C. Sutherland. 2012. The changing carbon cycle in the Southern Ocean. *Oceanography* 25(3):26–37, http://dx.doi.org/10.5670/oceanog.2012.71.

DOI

http://dx.doi.org/10.5670/oceanog.2012.71

THE CHANGING CARBON CYCLE IN THE SOUTHERN OCEAN

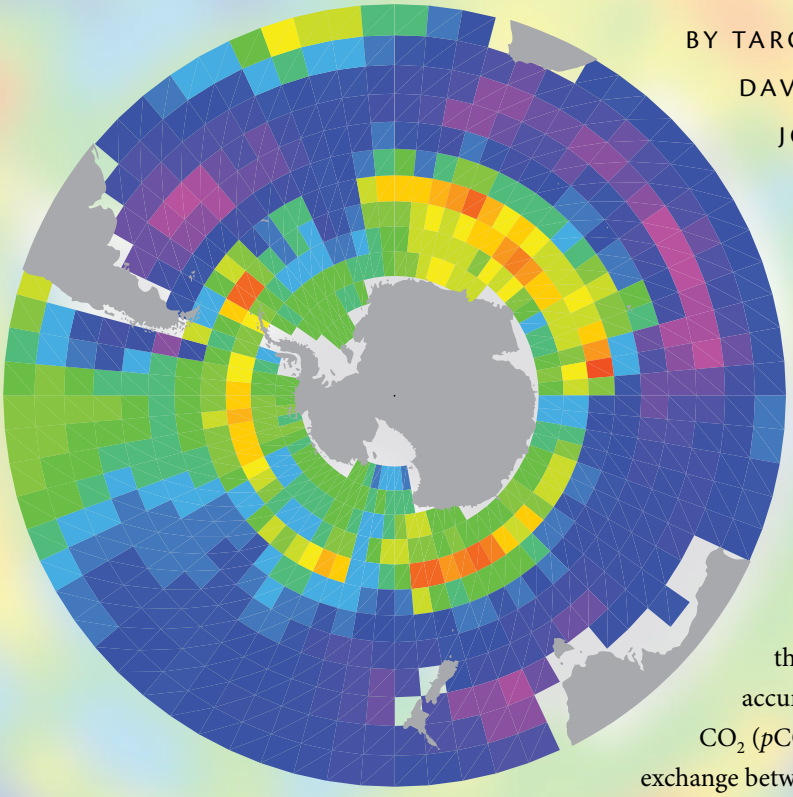

BY TARO TAKAHASHI, COLM SWEENEY, BURKE HALES, DAVID W. CHIPMAN, TIMOTHY NEWBERGER, JOHN G. GODDARD, RICHARD A. IANNUZZI, AND STEWART C. SUTHERLAND

ABSTRACT. Various human activities, including fossil fuel combustion and forest clearing, emit about eight petagrams (or billion tons) of carbon in the form of CO_2 into the atmosphere annually. The global ocean absorbs about two petagrams of CO_2, and about a half of that amount is absorbed by the Southern Ocean south of 30°S, thus slowing the rapid accumulation of CO_2 in the atmosphere. Partial pressure of CO_2 (pCO_2) is a measure of the chemical driving force for the CO_2 exchange between the ocean and the atmosphere. This paper discusses its space and time distribution over the Southern Ocean. The major sink zone for atmospheric CO_2 is located in a latitude belt between 30°S and 50°S, where the biological utilization of CO_2 and cooling of warm subtropical waters flowing southward produce low seawater pCO_2. Strong winds in this zone also enhance the ocean's uptake. Although the source-sink conditions vary over a wide range through the seasons in the areas south of 50°S, this zone is a small sink on an annual average. Winter observations show that surface water pCO_2 values in the source region for Antarctic Intermediate Water have increased at a rate faster than the atmospheric increase rate, suggesting that the ocean CO_2 sink intensity has been weakening for several decades and has changed from a net sink to a net source since 2005. The results of ocean general circulation-biogeochemistry model studies are found to be consistent with the observations.

INTRODUCTION

The Southern Ocean is a major region for the formation of deepwater masses that fill the ocean basins, and it is an important conduit for exchange of heat, momentum, and dissolved gases between the atmosphere and the ocean interior. The global ocean is currently absorbing annually about 2 Pg of carbon (1 Pg = 1 petagram = 10^{15} grams = 1 billion tons) from the air in the form of CO_2 gas, and the Southern Ocean south of 30°S takes up about 1 Pg of carbon. Thus, the Southern Ocean's significant role in the uptake and long-term storage of anthropogenic CO_2 emitted to the atmosphere affects Earth's climate.

The difference between the partial pressure of CO_2 (pCO_2) in seawater and that in the overlying air determines the direction of CO_2 transfer across the sea surface. Two opposing processes primarily govern CO_2 chemistry in seawater: sinking of biological products from the photic zone to deep-ocean regimes (i.e., the biological pump), and upward transport by upwelling deep waters of CO_2 and nutrients formed by the decomposition of biological debris. Thus, understanding the ocean's uptake rates of atmospheric CO_2 requires knowledge of ocean circulation dynamics as well as production and respiration dynamics in a wide range of ecosystems. A large number of observational and model studies have been conducted in recent years. The observational studies are based on the sea-air pCO_2 difference (Takahashi et al., 2009), $^{13}C/^{12}C$ mass balance (Quay et al., 2003), atmospheric oxygen and CO_2 changes (Bender et al., 2005; Manning and Keeling, 2006), and CO_2 change in the ocean (Sabine et al., 2004). The model studies include coupled Ocean General Circulation-Biogeochemistry models (OGCM) (Mikaloff-Fletcher et al., 2006; Sarmiento and Gruber, 2006; Jacobson et al., 2007; Lenton and Matear, 2007; Gruber et al., 2009; Le Quérér et al., 2010), and inversion of atmospheric CO_2 data using Atmospheric General Circulation models (AGCM) (Gurney et al., 2008). Gruber et al. (2009) reviewed the estimates for CO_2 uptake flux over the contemporary global ocean obtained by four groups of independent methods: inversion of the ocean data using 10 OGCMs, 13 ocean forward models (OCMIP-2), inversion of atmospheric CO_2 data (Gurney et al., 2008), and sea-air pCO_2 difference (Takahashi et al., 2009). Although the mean air-to-sea flux estimates for the contemporary global ocean obtained by these methods are in general agreement at 1.5 ± 0.5 Pg C yr^{-1}, notable discrepancies are found in the Southern Ocean. The ocean inversion methods suggest a relatively uniform weak sink in the areas south of 58°S, whereas the sea-air pCO_2 difference (ΔpCO_2) data in these areas suggest a CO_2 source. Processes governing atmosphere-ocean interactions in the Southern Ocean region are complex because of the large seasonal variability in temperature, wind regimes, ice/water conditions, and biological activities. Although significant progress has been made in recent years due to improved research facilities, observations are still limited because of operational difficulties related to hostile weather conditions, and observation-based estimates are subject to considerable uncertainty. Model results are also subject to uncertainties because of limited time-space resolutions and imperfections in the parameterizations for various processes, including eddy mixing, ice formation, and biological processes.

In this article, we review recent progress in biogeochemical studies on the carbon cycle with emphasis on the temporal and spatial variability of pCO_2 in Southern Ocean surface water. Here, the Southern Ocean is defined as the oceanic areas south of 30°S that include a major sink zone for atmospheric CO_2 centered at 40°S. First, we review climatological mean distribution of surface water pCO_2 and net sea-air CO_2 flux. Second, we discuss the change in surface water pCO_2 and the intensity of the ocean CO_2 sink in circumpolar waters.

Taro Takahashi *(taka@ldeo.columbia.edu) is Ewing Lamont Research Professor, Lamont-Doherty Earth Observatory of Columbia University, Palisades, NY, USA.* **Colm Sweeney** *is CIRES Research Scientist, Cooperative Research Institute in Environmental Sciences (CIRES), University of Colorado, Boulder, CO, USA.* **Burke Hales** *is Professor, College of Oceanic and Atmospheric Sciences, Oregon State University, Corvallis, OR, USA.* **David W. Chipman** *is retired from the Lamont-Doherty Earth Observatory of Columbia University, Palisades, NY, USA.* **Timothy Newberger** *is Associate, CIRES, University of Colorado, Boulder, CO, USA.* **John G. Goddard** *provides marine technical assistance for the Lamont-Doherty Earth Observatory of Columbia University, Palisades, NY, USA.* **Richard A. Iannuzzi** *is Intermediate Systems Analyst/Programmer, Lamont-Doherty Earth Observatory of Columbia University, Palisades, NY, USA.* **Stewart C. Sutherland** *is Research Staff Scientist, Lamont-Doherty Earth Observatory of Columbia University, Palisades, NY, USA.*

SEA-AIR CO_2 TRANSFER OVER THE SOUTHERN OCEAN

Before we discuss CO_2 exchange over the Southern Ocean, we briefly review relevant oceanographic information. Because pCO_2 is the primary quantity measured by our group, we next discuss the time-space distribution of surface water pCO_2, and then present the net sea-air CO_2 flux.

General Structure of the Upper Waters

The oceanographic features in the Southern Ocean are primarily zonal due to strong, persistent westerly winds blowing around the Antarctic Continent. Several oceanographically distinct zones are separated by fronts where water properties change (Orsi et al., 1995): from north to south, these are the Subtropical Front (STF), the Subantarctic Front (SAF), the Polar Front (PF), the Antarctic Divergence (AD), and the Continental Water Boundary (CWB). The Antarctic Circumpolar Current (ACC) includes the waters south of STF and north of CWB. Figure 1a shows the approximate positions of these fronts. In the high-latitude areas (60°S–70°S), high-salinity water (Lower Circumpolar Deep Water, LCDW, with a salinity of ~ 34.68) upwells along the Antarctic Divergence (AD). As the upwelled water drifts northward, it is altered by exchange with air, and it is subducted along the Polar Front (PF; 50°S–60°S). In general, high-latitude Southern Ocean surface waters are high in nutrients and CO_2 but low in chlorophyll concentrations (called HNLC conditions), with the exception of local waters in the coastal zone around Antarctica. The high concentrations of nutrients and CO_2 are due to the wintertime convective mixing of Upper Circumpolar Deep Water (UCDW) rich in CO_2 and nutrients as well as northward Ekman transport of the upwelled deep waters. In the vicinity of the Sub-Antarctic front (SAF; 50°S–55°S), low-salinity Intermediate Water (AAIW, temperatures 3°–5°C, salinity about 34.3) is formed and sinks to the base of the main thermocline (~ 900 m deep). Further north, along the Subtropical Front (~ 40°S), the sub-Antarctic surface water that is replete with nutrients but low in chlorophyll (i.e., HNLC) converges with warm subtropical surface water that is depleted in nutrients. In the resulting high primary productivity zone that is clearly visible in satellite color images (Moore and Abbott, 2000), surface water pCO_2 is reduced, creating a strong CO_2 sink zone centered around 40°S in the Atlantic, Indian, and most of the Pacific Oceans. These waters (Mode Water) sink to mid-depth and transport atmospheric CO_2 to the subsurface regime.

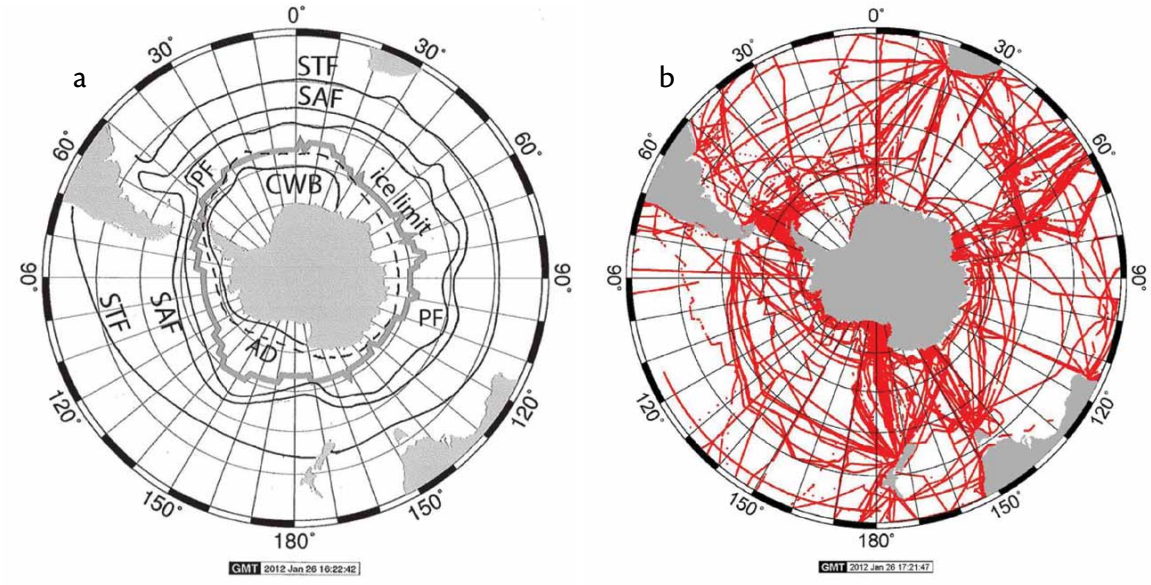

Figure 1. (a) Zonal structure of Southern Ocean surface waters (based on Orsi et al., 1995), showing the approximate locations of fronts: STF = Subtropical Front. SAF = Subantarctic front. PF = Polar Front. AD = Antarctic Divergence. CWB = Continental Water Boundary. Winter ice limit is indicated with a broad gray curve. (b) Locations of surface water pCO_2 measurements between 1960 and 2011 over the Southern Ocean. Approximately 2.1 million pCO_2 measurements were made during this period; the data (Takahashi et al., 2011) are available at the Carbon Dioxide Information and Analysis Center at Oak Ridge National Laboratory (CDIAC; http://cdiac.ornl.gov/oceans/LDEO_Underway_Database).

CO_2 Partial Pressure in Surface Water

In seawater, CO_2 molecules exist in three forms: as CO_2 molecules in an aqueous environment ($[CO_2]_{aq}$ or $[H_2CO_3]$) and as two ionized forms ($[HCO_3^-]$ and $[CO_3^=]$). The sum of these species is referred to as the total concentration of CO_2 dissolved in seawater (TCO_2), which is measured as the total amount of CO_2 extracted from an acidified seawater sample. In surface ocean waters, about 1% of TCO_2 exists as $[CO_2]_{aq}$, about 4% as $[CO_3^=]$, and 95% as $[HCO_3^-]$. Of these, $[CO_2]_{aq}$ is the only species involved in the exchange of CO_2 between the sea and the overlying air. The partial pressure of seawater CO_2 is a measure of $[CO_2]_{aq}$, and represents the driving force for the transfer of CO_2 gas across the sea-air interface. The difference between pCO_2 in seawater and air (ΔpCO_2) determines the direction and magnitude of the net CO_2 flux across the interface. When the pCO_2 in seawater is greater than that in the overlying air ($\Delta pCO_2 > 0$), the net flux is from sea to air; when $\Delta pCO_2 < 0$, the net flux is from air to sea. The net sea-air flux may be estimated by multiplying the sea-air pCO_2 difference by the gas transfer coefficient across the sea surface.

Observations of Surface Water pCO_2

Figure 1b shows the locations of where surface water pCO_2 data have been collected over the Southern Ocean since the 1960s. The observations were made using a gas-seawater equilibrator coupled with a CO_2 analyzer (gas chromatograph or IR analyzer) that was calibrated using three or more certified CO_2-air reference gas mixtures by the Climate Monitoring and Diagnostics Laboratory of the National Oceanic and Atmospheric Administration (NOAA), Boulder, CO. Equilibrators (bubbler, membrane, or shower types; e.g., Chipman et al., 1993; Hales et al., 2004; Newberger, 2004) were operated either in a seawater flow-through mode for continuous underway measurement of water samples pumped from an intake located a few meters below the sea surface, or in a discrete water mode for water samples collected in nonmetallic sampling bottles. Seawater temperature and salinity and equilibration pressure and temperature are recorded and used for computing in situ pCO_2 values. The overall precision of the pCO_2 data is estimated to be ± 2 µatm.

Climatological Mean Distribution of Surface Water pCO_2

Figure 2 displays monthly distribution maps for the climatological mean sea-air pCO_2 difference for the reference year 2000. Here, we briefly describe the method used for constructing these maps. Because pCO_2 has increased with time in response to the increase in atmospheric CO_2, data obtained in different years and months are corrected to a reference year 2000 using a mean rate of 1.5 µatm yr^{-1}, which is assumed to be equal to the mean atmospheric CO_2 increase. The corrected pCO_2 values are binned into 4° x 5° boxes, and monthly mean values for each box are computed. Because fewer than 50% of the boxes have observations, they are interpolated using a two-dimensional diffusion-advection transport equation to fill all the boxes. The sea-air pCO_2 differences (ΔpCO_2) are computed using atmospheric pCO_2 values that are calculated from zonal mean atmospheric CO_2 concentrations in dry air for the year 2000 (GLOBALVIEW, 2006) and monthly mean values for barometric pressure and water vapor pressure at the sea surface. The computational details are described in Takahashi et al. (2009), and the climatological mean values in each box are available at http://www.ldeo.columbia.edu/res/pi/CO2.

Figure 2 shows that a strong CO_2 sink zone (blue color with negative ΔpCO_2) is located near 40°S during the austral winter months (June through October). Its formation is attributed primarily to high productivity in the high-chlorophyll zone observed by satellites over the same latitudes (see Plates 3 and 6 in Moore and Abbott, 2000). However, the colocation of the CO_2 sink zone and the high-productivity zone is only qualitative because seawater pCO_2 is governed by net community production, which includes primary production as well as the respiration, recycling, and export of organic carbon from the mixed layer. Peaking of the sink intensity in August and September suggests that winter cooling of surface water plays an important role in the formation of the sink. As the season progresses, the CO_2 sink zone moves southward due mainly to increased photosynthesis under longer daylight hours and warmer temperatures. The biological drawdown effect is clearly seen in the areas north of the Weddell and Ross Seas, where satellites observe high concentrations of chlorophyll (see Plate 3 of Moore and Abbott, 2000). Boutin et al. (2008) measured sea-air pCO_2 difference continuously in the zone between the PF and the SAF (40°S–55°S) in the Pacific and Indian Ocean sectors using the CARIOCA

(Carbon Interface Ocean Atmosphere) drifter buoys during all seasons from 2001 to 2006, observing that the waters in these areas are mostly undersaturated with a mean ΔpCO_2 of −19 µatm. Their mean value is similar to our climatological mean within about 2 µatm.

In the permanently open ocean zone (POOZ) of the ACC between 50°S and 60°S, ΔpCO_2 is generally small (light blue and green in Figure 2) because of the competing effects of temperature and TCO_2 on seawater pCO_2: summertime photosynthesis reduces TCO_2 and pCO_2, counteracting pCO_2 increase due to warming, whereas wintertime cooling counteracts the increasing effect on pCO_2 of upwelled high TCO_2 deep waters. In the Indian Ocean sector between 50°S and 58°S, Metzl et al. (2006) measured pCO_2, TCO_2, alkalinity, and the concentrations of chlorophyll, silicate, and nitrate during January and August cruises in

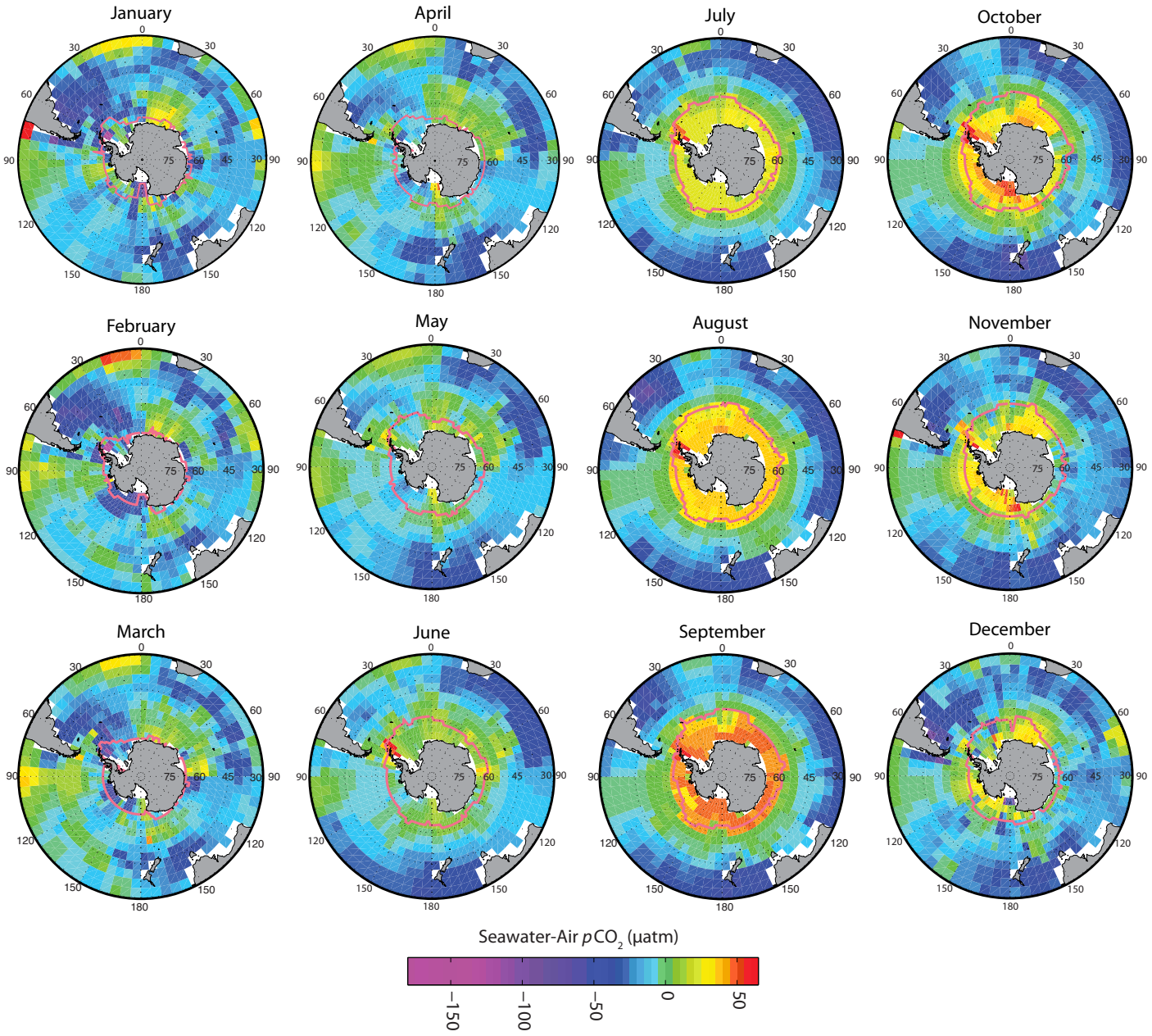

Figure 2. Monthly distribution maps for the climatological mean sea-air pCO_2 difference (µatm) for the reference year 2000. The pink curves indicate the approximate locations of the northern edges of ice fields, and hence define the seasonal ice zone. The high pCO_2 values in the under-ice mixed layer are due to the upward mixing of high CO_2 Upper Circumpolar Deep Water.

2000, observing that the summertime seawater pCO_2 was lower than the atmospheric pCO_2 (ΔpCO_2 ~ –15 µatm) due to photosynthesis, and the winter pCO_2 was higher than the atmospheric (ΔpCO_2 ~ +10 µatm) due to the upwelling of high-CO_2 deep waters. Because the alkalinity was found to be similar, the biological effect on CO_2 is due mostly to the production of organic carbon.

In the seasonal ice zone (SIZ, south of ~ 60°S, poleward of the "ice limit" curve in Figure 1 and poleward of the pink curves in Figure 2), the seawater in autumn has low pCO_2 values because of biological utilization during the preceding season. As the sea ice field develops, a mixed layer of seawater forms under the ice field, and its CO_2 and nutrient concentrations increase as deep waters are mixed into it as the seasons progress. As Figure 3 shows, the pCO_2 in ice field waters is low (~ 340 µatm) soon after the formation of the ice in June (day 170), and it increases during the progressing winter season to about 420 µatm in September (day 260). Although algae grow in the basal zone of sea ice, their photosynthetic utilization of CO_2 is slow because of low light conditions due to winter darkness and ice-snow cover (Lizotte, 2001; Arrigo and Thomas, 2004), and it does not significantly reduce the large amount of CO_2 dissolved in a thick under-ice mixed layer. From mid-July through September, pCO_2 in the under-ice waters exceeds the atmospheric pCO_2, and therefore, the under-ice water CO_2 is released to the air when the water is exposed to the air. In the early spring, as sea ice fields start to break up, the water in the marginal ice zone (MIZ) should be a CO_2 source. When the winter sea ice thins and melts away in the spring, phytoplankton blooms, fueled by high nutrient concentrations, reduce the pCO_2 in water, and the water rapidly becomes a sink for atmospheric CO_2, as Bakker et al. (2008) observe in the Weddell Sea area. The transition from CO_2 source to sink occurs as the ice fields retreat in the spring, sweeping across the 15×10^6 km^2 SIZ of the Southern Ocean.

The coastal waters reflect the properties of upwelled waters modified by complex shelf processes, and they regulate the transport of atmospheric CO_2 into the deep and abyssal regimes (see Takahashi and Chipman, 2012, in this issue). In summer, the Ross and Weddell Seas and the coastal waters in the Amundsen and Bellingshausen Seas are strong CO_2 sinks with pCO_2 values as low as 170 µatm (~ 210 µatm below the air pCO_2) due to intense photosynthesis, whereas they are a strong source during winter with pCO_2 as high as 425 µatm (~ 45 µatm above the present air pCO_2) due to upwelling of high-CO_2 deep waters (Bakker et al., 1997, 2008; Bates et al., 1998; Rubin et al., 1998; Sweeney, 2003; Hales and Takahashi, 2004; Rubin, 2003; Arrigo and van Dijken, 2007).

Net Sea-Air CO_2 Flux from ΔpCO_2

The net CO_2 flux across the sea surface ($F_{sea\text{-}air}$) may be estimated by Equation 1, in which the main drivers are wind speed and sea-air pCO_2 difference (ΔpCO_2):

$$F_{sea\text{-}air}\ (\text{g C m}^{-2}\ \text{month}^{-1}) = 0.585 \cdot \text{Ko} \cdot (\text{Sc})^{-1/2} \cdot (\text{U}_{10})^2 \cdot \Delta pCO_2, \quad (1)$$

where Ko is the solubility of CO_2 in seawater (mol CO_2 liter^{-1} atm^{-1}; Weiss, 1974), Sc is the Schmidt number (see Wanninkhof, 1992), U_{10} (m sec^{-1}) is the wind speed at 10 m above the sea surface, and ΔpCO_2 is in µatm. The number 0.585 includes a unit conversion factor (changes from second to month, from liter to m^3), the gas

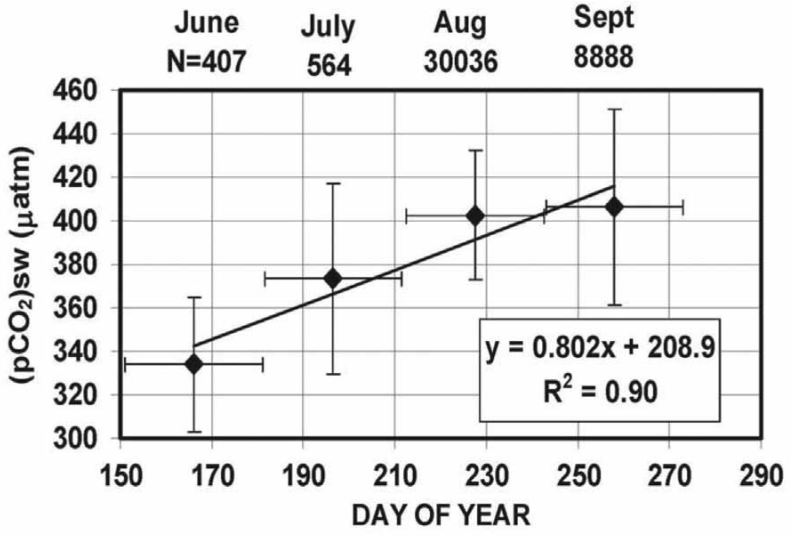

Figure 3. Seawater pCO_2 observed in ice field waters with temperatures less than –1.75°C in areas south of 60°S during June to September since 1998. The measurements were made possible by improvements in the intake port for the scientific water sampling line aboard RVIB *Nathaniel B. Palmer* that prevent ice clogging. The data obtained in different years are averaged for each month, and one standard deviation is shown. The pCO_2 in under-ice water increases as the season progresses. *From Takahashi et al. (2009)*

transfer scaling factor of 0.26, and the reference Schmidt number of $(660)^{1/2}$ at 20°C for seawater (Takahashi et al., 2009). Although Ko and Sc vary with temperature, the temperature effects cancel in the ratio, and $Ko/(Sc)^{1/2}$ is nearly constant in the ocean temperature range. The 0.26 (± 30%) scaling factor for the gas transfer rate is determined using the bomb carbon-14 data with the Geophysical Fluid Dynamics Laboratory Ocean General Circulation Model (GFDL OGCM; Sweeney et al., 2007) specifically for the 1979–2005 NCEP-DOE AMIP-II Reanalysis six-hour wind data (Kanamitsu et al., 2002), which are used in this study. Several wind speed products are available for the global ocean, and they vary considerably. Hence, the estimated flux varies by about 20%, depending on the wind speed product used (Signorini and McClain, 2009).

Climatological Mean Sea-Air CO_2 Flux

Figure 4 shows the meridional distribution of climatological mean CO_2 flux over the global ocean in the reference year 2000, which yields a net global ocean CO_2 uptake flux of 1.6 ± 0.7 Pg C yr^{-1}. Although the flux uncertainty from the error in ΔpCO_2 is relatively small (13%), the errors in the scaling factor for the gas transfer rate formula (± 30%) and the wind speed variability (± 20%) are major contributors to the flux uncertainty (Takahashi et al., 2009). The equatorial waters are the major CO_2 source of about 0.7 Pg C yr^{-1}. This source is counteracted by the two major sinks: a 1.0 Pg C yr^{-1} sink centered around 40°S in the Southern Hemisphere and a 0.7 Pg C yr^{-1} sink centered around 40°N in the Northern Hemisphere. Thus, the Southern Ocean plays a significant role in the global ocean CO_2 cycle.

Figure 5 shows the climatological mean distributions of CO_2 flux for February and August, and the annual average in the reference year 2000. During the austral summer (February), a belt of strong sink is centered around 45°S. This sink is especially robust in the Atlantic sector, perhaps due to intense mixing caused by rough topography and the confluence of warm subtropical and nutrient rich sub-Antarctic waters. Shallow mixed layers in this area (Dong et al., 2008) also enhance the effect of biological drawdown. Intense sink areas are also found in the Ross Sea gyre area, attributed primarily to biological drawdown of pCO_2 fueled by abundant nutrients and sunlight. The zones south of about 50°S and north of about 40°S are neutral (green) or weak source areas (yellow), reflecting the small ΔpCO_2 that results from compensating effects of warming and increased biological CO_2 utilization.

During the austral winter (August), wind intensifies and water cools, causing the sink zone centered around 40°S to intensify. The gas transfer rate is increased as a square function of wind speed (Equation 1), and the cooling reduces surface water pCO_2, although these effects are partially compensated by the increased pCO_2 of upwelling of deep waters. The neutral zone (green) south of the sink zone expands, perhaps due to the increase in deepwater upwelling. In the sea ice zone south of about 55°S, the sea-air CO_2 flux is computed assuming that a layer of solid ice blocks gas exchange and that sea-air gas exchange takes place only through open water areas in ice fields. For the open water areas, the CO_2 flux is computed using Equation 1, in

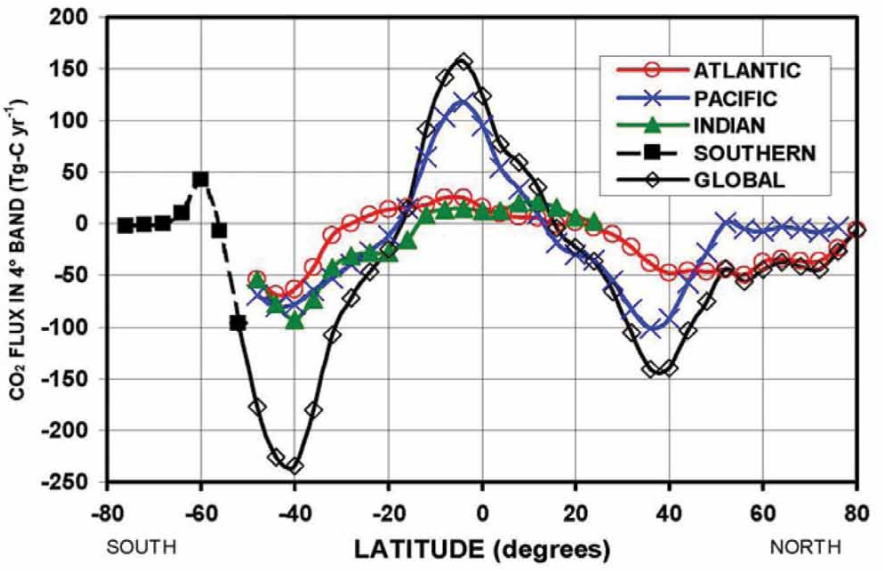

Figure 4. Climatological mean sea-air CO_2 flux in 4° zonal bands in the four major ocean basins in the reference year 2000. The flux values are expressed in Tg C yr^{-1} (Tg = teragrams = 10^{12} grams = million tons) for each 4°-wide zonal band across each ocean basin. This plot gives a total global air-to-sea flux of 1.6 Pg C yr^{-1}. The wind speed data are from the 1979–2005 NCEP-DOE AMIP-II Reanalysis, and the gas transfer coefficient is computed using Equation 1. *From Takahashi et al. (2009)*

which the ΔpCO_2 is represented by ice field measurements shown in Figure 3. In June, the ΔpCO_2 in under-ice waters is negative, reflecting the low pCO_2 conditions produced by the biological pump during the preceding months. Hence, when water is exposed to the air, it acts as a sink for atmospheric CO_2, and as the season progresses, it becomes a source by July. For the ice field surrounding the continent, the NCEP/DOE 2 Reanalysis (2005) ice cover data are regridded to our 4° x 5° grid and averaged for each month. When the ice cover is less than 10% in a 4° x 5° box area, it is assumed to be all water. Between 10% and 90%, the flux is computed proportional to the water area. Because ice fields have leads and polynyas due to dynamic motion of sea ice, we assume the fields to be 10% open water even though the satellite data report 100% ice cover (Worby et al., 2008). The strong CO_2 source zone centered around 60°S (yellow-orange) reflects the ice field edge zone in late winter months, when a large area of seawater with positive ΔpCO_2 values is exposed to the air, allowing gas exchange. Although the seasonal ice zone exhibits large seasonal changes in physical, biological, and chemical conditions, this zone appears to make a small contribution in terms of annual sea-air CO_2 flux to the global sea-air CO_2 budget.

On the annual mean, the zone centered around 40°S (magenta-blue; sea surface temperature [SST] between 10°C and 15°C) stands out as a prominent sink for the global sea-air carbon budget. To investigate Southern Ocean CO_2 uptake and its relationship to the Southern Annular Mode (SAM), Lovenduski et al. (2007) used the forward Parallel Ocean Program Ocean GCM coupled with a biogeochemical-ecological model. They found strong CO_2 sink zones centered around 40°S, and they determined that the sink in the Atlantic and the western Indian Ocean sectors were most intense and the southeastern Pacific less so. Their model results for the distribution and magnitude of the CO_2 sink/source in the contemporary ocean (see their Figure 3a) are in good agreement with our results in the "Annual" panel in Figure 5. The Ocean GCM results obtained by Lenton and Matear (2007) also exhibit a strong CO_2 sink zone around 40°S. However, the distribution patterns are somewhat different from our results: the sink zone is strongest in the Pacific and Indian Ocean sectors, while it is much weaker in the Atlantic sector.

CHANGE OF THE SOUTHERN OCEAN CO_2 SINK/SOURCE

Whether the CO_2 sink intensity in the Southern Ocean has changed in recent decades in response to increasing atmospheric loading of CO_2 and

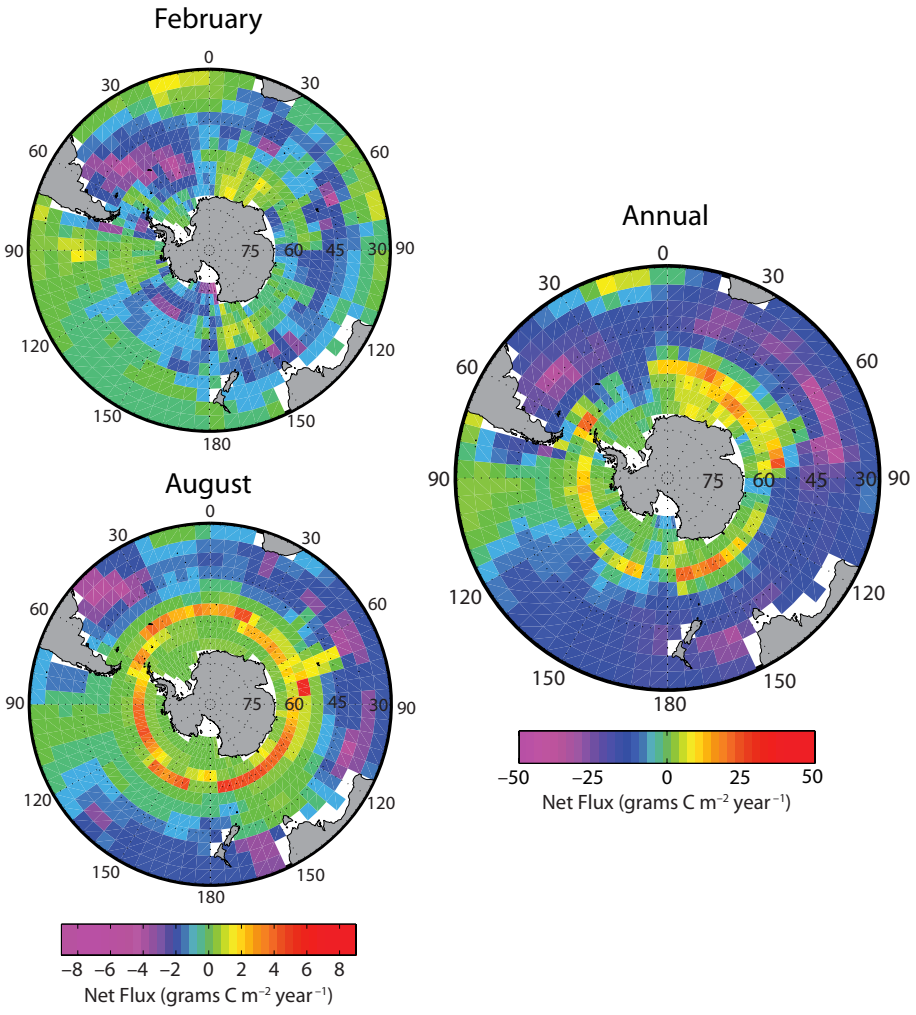

Figure 5. Distribution of climatological mean sea-air CO_2 flux in the reference year 2000 for February and August, along with the annual mean. See text for the assumptions used for estimating the flux in the sea ice fields. The source zone is indicated with yellow and orange, the sink zone with blue and magenta, and the neutral (small flux) zone with green.

climate change is an important question. This issue has been addressed actively in recent GCM studies. Le Quéré et al. (2007) inverted the atmospheric CO_2 concentration data from 12 stations located south of 30°S to obtain sea-air CO_2 flux, and observed that the Southern Ocean CO_2 sink weakened during 1981–2004. They attributed this weakening to the increase in upwelling of deep waters caused by stronger winds during this period. Le Quéré et al. (2010) used a forward Ocean GCM coupled with a marine biogeochemistry model to investigate the contributions of temperature, atmospheric CO_2, wind regimes, and heat-water flux to the sea-air CO_2 flux using three different wind products. They found that regional differences in the annual rates for sea-air pCO_2 change developed only when the model was driven using both increasing atmospheric CO_2 and changing climate. Their model study yielded a mean decadal rate of ΔpCO_2 change of about 20 µatm decade^{-1}, which is about 4 µatm decade^{-1} faster than the mean atmospheric CO_2 increase rate of about 16 µatm decade^{-1} for their study period of 1981–2007. Lenton and Matear (2007) and Lovenduski et al. (2007) used Biogeochemistry-Ocean GCMs to explore the relationship between the SAM and changes in the Southern Ocean CO_2 flux. These investigators found that the southward shift and the intensification of zonal winds that occurred during the positive trend of SAM for the past several decades caused an increase in deepwater upwelling, which in turn increased surface water pCO_2 and decreased CO_2 sink intensity. The magnitudes of changes estimated by these model studies are broadly in agreement.

Circumpolar Open Water Zone

To document how the primary driving force of CO_2 uptake over the Southern Ocean has changed in recent decades, we analyzed the wintertime data for surface water pCO_2 in the open ocean water zone, which includes the AAIW formation areas. Because biological activities are minimal and the vertical mixing of water is expected to be maximal during the winter months, the trend in winter surface water pCO_2 should indicate the trends in vertical mixing and possibly meridional transport rate. Furthermore, the time trend must be evaluated based on the pCO_2 time-series values of a similar water mass or type. We have chosen wintertime SST as the indicator, and divided the data into five temperature zones between 0.8°C and 5.5°C. Figure 6 shows the time plots and data locations, and Table 1 summarizes the results of linear regression analysis for pCO_2 and SST in each zone. The pCO_2 rates that are corrected for changes in SST are also listed. While the rates for the coldest and warmest zones (0.80°–1.5°C and 4.5°–5.5°C, respectively) are similar to the atmospheric rate, the middle three zones (1.5°–4.5°C, about 50°–55°S) have significantly faster rates (23.9 ± 3.8 µatm decade^{-1}) than the atmospheric rate of about 16 µatm decade^{-1}, indicating that the ocean CO_2 uptake is weakening. The faster increase in seawater pCO_2 compared to atmospheric pCO_2 means that this zone, which had been a sink for atmospheric CO_2 since the beginning of our measurements in the 1960s, changed to a source some time after 2005. In 1960, the atmospheric pCO_2 was about 310 µatm (CO_2 concentration in dry air of 316 ppm corrected for the barometric pressure and water vapor), whereas the seawater pCO_2 was between 275 and 300 µatm, 10 to 35 µatm below the atmospheric. In contrast, the atmospheric pCO_2 was about 377 µatm (385 ppm CO_2 in dry air) in 2010, and the seawater pCO_2 was 375 to 385 µatm, equal or slightly greater than the atmospheric value.

Importantly, this temperature zone corresponds to the formation region for the AAIW, and the observed high rate of pCO_2 increase suggests a reduction of the CO_2 sink intensity for AAIW due to an increase in upwelling of CO_2-rich deep waters. Although the validity of the eddy mixing parameterizations used in the ocean model studies has been questioned by Böning et al. (2008) and Downs et al. (2011), Le Quéré et al.'s (2010) estimate of 20 µatm decade^{-1} (when the model results are sampled at the same location and time as the observations) is consistent with our observations.

Changes in the intense CO_2 sink zone centered around 40°S are clearly important for projecting future global ocean CO_2 uptake. However, presently available pCO_2 data are not extensive enough to address this issue reliably. For example, Metzl (2009) investigated changes in the intense CO_2 sink zone in the southern Indian Ocean and reported a 1991–2007 mean winter rate of increase ranging between 36 ± 4 and 47 ± 10 µatm decade^{-1} (corrected for SST change) in the southern half of the sink zone between 40°S and 55°S; this indicates a weakening of the sink intensity due to much faster rates of oceanic pCO_2 increase than the atmospheric rate of 16 µatm decade^{-1}. On the other hand, a much lower rate of 6 µatm yr^{-1} was

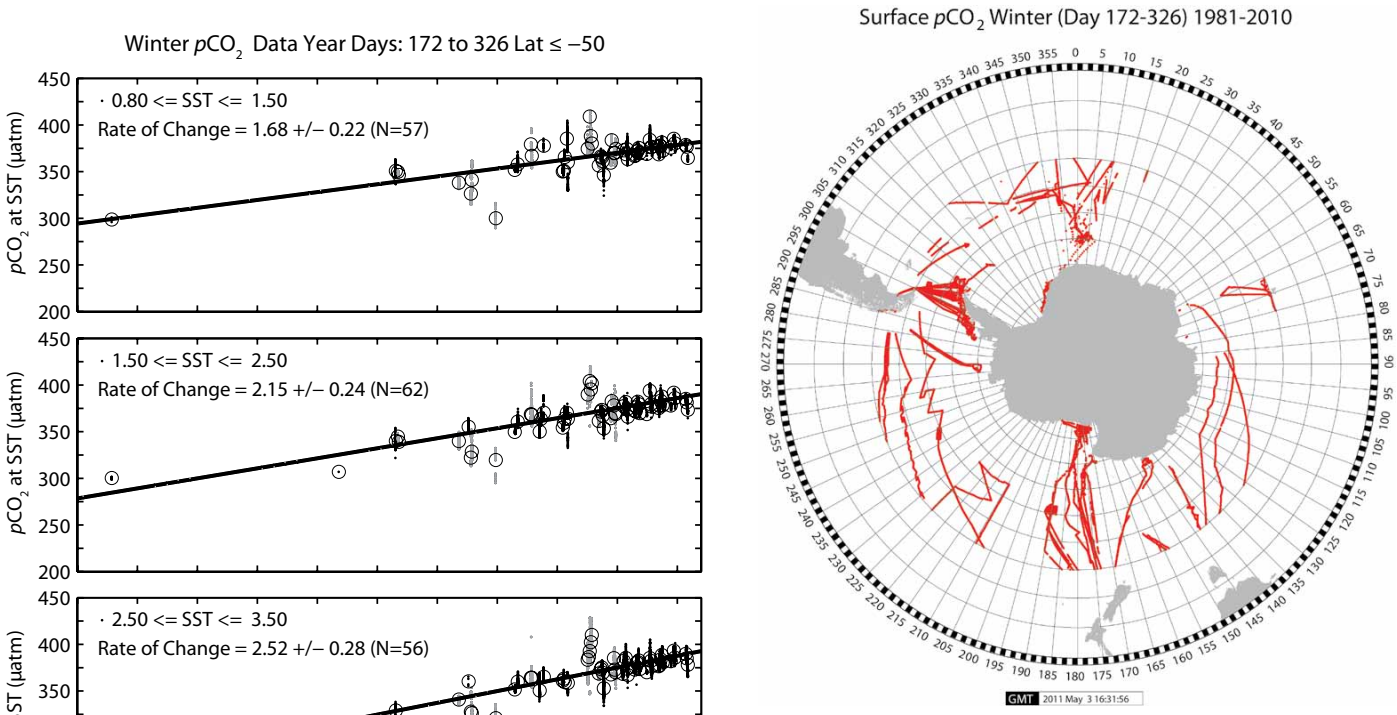

Figure 6. Sample locations and the time trend of surface water pCO_2 data during the winter months (year days 172–326). The mean rate of change is shown with the heavy black linear regression line and the values in the unit of µatm yr^{-1}. The data collected during the El Niño and non-El Niño periods are shown, respectively, with gray and black dots. The open circles are monthly means, used for linear regression calculations. The data are available at CDIAC. *From Takahashi et al. (2011)*

Table 1. The mean decadal rate of change for wintertime surface water pCO_2 and sea surface temperature (SST) in five temperature zones. The second column shows the mean rate of pCO_2 change as observed in Figure 6, and the SST change in the third column is estimated using the temperature data obtained concurrently with the pCO_2 data. The fourth column shows the pCO_2 change corrected for the SST change using 4.23% pCO_2 change per °C.

SST Range (°C)	pCO_2 Change µatm $decade^{-1}$ (1986–2010)	SST Change °C $decade^{-1}$ (1986–2010)	pCO_2 Change corrected for SST µatm $decade^{-1}$	No. of Months	Data Counts
0.80–1.50	16.8 ± 2.9	-0.031 ± 0.021	17.3 ± 3.2	56	4,668
1.50–2.50	23.8 ± 3.0	+0.020 ± 0.028	23.5 ± 3.4	61	9,326
2.50–3.50	25.2 ± 2.8	+0.13 ±0.038	23.3 ± 3.4	56	12,473
3.50–4.50	24.3 ± 4.2	−0.045 ± 0.036	24.9 ± 4.7	59	19,163
4.50–5.50	16.7 ± 2.8	+0.031 ± 0.034	16.2 ± 3.3	59	24,114
----------	----------	----------	----------	----	--------
0.80–5.50	21.4 ± 4.2	0.02 ± 0.03	21.0 ± 3.4	288	69,744
1.50–4.50	24.4 ± 3.3	0.04 ± 0.09	23.9 ± 3.8	176	40,962

observed in the northern half between 35°S and 40°S, suggesting an increase in sink intensity. More observations are needed to document the change in this important sink zone.

CONCLUSION

The global ocean is currently absorbing annually about 2 Pg C yr^{-1} of CO_2 from the air, and it plays a significant role in the uptake and long-term storage of anthropogenic CO_2 that is emitted to the atmosphere, affecting Earth's climate. The climatological mean sea-air flux is estimated by the observed sea-air pCO_2 difference and the gas transfer rate parameterized as a function of (wind speed)^2. A Southern Ocean zone between 30°S and 50°S is found to be a major sink for atmospheric CO_2, taking up 1.0 Pg C yr^{-1}. Thus, the Southern Ocean is a major ocean sink for atmospheric CO_2. This paper discusses how this CO_2 sink is changing in response to recent climate change.

We investigated the multidecadal mean trends for surface water pCO_2 and temperature (0.8°–5.5°C) during winter in the formation region for AAIW. The wintertime waters were chosen because of minimal winter biological activity in order to avoid large biologically induced variability in seawater pCO_2, and because of the maximal vertical mixing. The pCO_2 in the waters between 1.5°C and 4.5°C has increased at a rate of 23.9 ± 3.8 µatm $decade^{-1}$, which is faster than the rate of atmospheric pCO_2 increase of about 16 µatm $decade^{-1}$. This suggests weakening CO_2 sink intensity for AAIW, which transports water to depths of about 900 m. The rate of change in the intense CO_2 sink zone centered at about 40°S is clearly important, but it cannot be determined reliably due to limited observations. The observed distribution and the mean rate of change in surface water pCO_2 of the Southern Ocean are generally in agreement with the results of the Biogeochemistry-Ocean GCM studies.

ACKNOWLEDGMENTS

This study was supported by grants from NOAA (NA080AR4320754) and NSF (ANT06-36879). We benefited greatly from advice offered by Douglas Martinson, Stanley Jacobs, and Arnold L. Gordon of Lamont-Doherty Earth Observatory. We gratefully acknowledge the dedicated operational assistance provided by the ships' captains and crews aboard the research vessels *Nathaniel B. Palmer*, *Laurence M. Gould*, *Akademik Ioffe*, *Marion-Dufresne*, and other ships, who helped us to make observations. We are particularly grateful for valuable technical assistance provided by Raytheon Antarctic Services.

REFERENCES

Arrigo, K.R., and D.N. Thomas. 2004. Large scale importance of sea ice biology in the Southern Ocean. *Antarctic Science* 16(4):471–486, http://dx.doi.org/10.1017/S0954102004002263.

Arrigo, K.R., and G.L. van Dijken. 2007. Interannual variation in air-sea flux in the Ross Sea, Antarctica: A model analysis. *Journal of Geophysical Research* 112, http://dx.doi.org/10.1029/2006JC003492.

Bakker, D.C.E., M. Hoppema, M. Schröder, W. Geibert, and H.J.W. de Baar. 2008. A rapid transition from ice covered CO_2–rich waters to a biologically mediated CO_2 sink in the eastern Weddell Gyre. *Biogeosciences Discussions* 5:1,205–1,235, http://dx.doi.org/10.5194/bgd-5-1205-2008.

Bakker, D.C.E., H.J.W. de Baar, and U.V. Bathmann. 1997. Changes of carbon dioxide in surface waters during spring in the Southern Ocean. *Deep-Sea Research Part II* 44:91–127, http://dx.doi.org/10.1016/S0967-0645(96)00075-6.

Bates, N.R., D.A. Hansell, C.A. Carlson, and L.I. Gordon. 1998. Distribution of CO_2 species, estimates of net community production and sea-air CO_2 exchange in the Ross Sea polynya. *Journal of Geophysical Research* 103(C2):2,883–2,896, http://dx.doi.org/10.1029/97JC02473.

Bender, M.L., D.T. Ho, M.B. Hendricks, R. Mika, M.O. Battle, P.P. Tans, T.J. Conway, B. Sturtevant, and N. Cassar. 2005. Atmospheric O_2/N_2 changes, 1993–2002: Implications for the partitioning of fossil fuel CO_2 sequestration. *Global Biogeochemical Cycles* 19, GB4017, http://dx.doi.org/10.1029/2004GB002410.

Böning, C.W., A. Disper, M. Visbeck, S.R. Rintoul, and F.U. Schwartzkopf. 2008. The response of the Antarctic Circumpolar Current to recent climate change. *Nature Geoscience* 1:864–869, http://dx.doi.org/10.1038/ngeo362.

Boutin, J., L. Merlivat, C. Henocq, N. Martin, and J.B. Sallee. 2008. Air-sea CO_2 flux variability in frontal regions of the Southern Ocean from CARbon Interface OCean Atmosphere drifters. *Limnology and Oceanography* 53(5, part 2):2,062–2,079, http://dx.doi.org/10.4319/lo.2008.53.5_part_2.2062.

Chipman, D.W., J. Marra, and T. Takahashi. 1993. Primary production at 47°N and 20°W in the North Atlantic Ocean: A comparison between the ^{14}C incubation method and the mixed layer carbon budget. *Deep-Sea Research Part II* 40(1/2):151–169, http://dx.doi.org/10.1016/0967-0645(93)90011-B.

Dong, S., J. Sprintall, S.T. Gille, and L. Talley. 2008. Southern Ocean mixed-layer depth from Argo float profiles. *Journal of Geophysical Research* 113, C06013, http://dx.doi.org/10.1029/2006JC004051.

Downs, S.M., A. Gnanadesikan, S. Griffies, and J.L. Sarmiento. 2011. Water mass exchange in the Southern Ocean in coupled climate models. *Journal of Physical Oceanography* 41:1,756–1,771, http://journals.ametsoc.org/doi/abs/10.1175/2011jpo4586.1.

GLOBALVIEW-CO_2 (Cooperative Atmospheric Data Integration Project - Carbon Dioxide). 2006. CD-ROM, NOAA CMDL, Boulder, Colorado. (Also available on Internet via anonymous FTP to ftp.cmdl.noaa.gov, Path: ccg/co2/GLOBALVIEW.)

Gruber, N., M. Gloor, S.E. Mikaloff Fletcher, S.C. Doney, S. Dutkeiwicz, M.J. Follows, M. Gerber, A.R. Jacobson, F. Joos, K. Lindsay, and others. 2009. Oceanic sources, sinks, and transport of atmospheric CO_2. *Global Biogeochemical Cycles* 23, GB1005, http://dx.doi.org/10.1029/2008GB003349.

Gurney, K.R., D. Baker, P. Rayner, A.S. Denning, and TransCom 3 L2 modelers. 2008. Interannual variations in regional net carbon exchange and sensitivity to observing networks estimated from atmospheric CO2 inversions for the period 1979 to 2006. *Global Biogeochemical Cycles*, 22, GB3025, http://dx.doi.org/10.1029/2007GB003082.

Hales, B., D.W. Chipman, and T. Takahashi. 2004. High-frequency measurement of partial pressure and total concentration of carbon dioxide in seawater using microporous hydrophobic membrane contactors. *Limnology and Oceanography Methods* 2:356–364, http://dx.doi.org/10.4319/lom.2004.2.91.

Hales, B., and T. Takahashi. 2004. High-resolution biogeochemical investigation of the Ross Sea, Antarctica, during the AESOPS (U.S. JGOFS) Program. *Global Biogeochemical Cycles* 18, GB3006, http://dx.doi.org/10.1029/2003GB002165.

Jacobson, A.R., S.E. Mikaloff Fletcher, N. Gruber, J.L. Sarmiento, and M. Gloor. 2007. A joint atmosphere-ocean inversion for surface fluxes of carbon dioxide. Part 2: Regional results. *Global Biogeochemical Cycles* 21, GB1020, http://dx.doi.org/10.1029/2006GB002703.

Kanamitsu, M., W. Ebisuzaki, J. Woollen, S.-K. Yang, J.J. Hnilo, M. Fiorino, and G.L. Potter. 2002. NCEP-DOE AMIP-II Reanalysis (R-2). *Bulletin of the American Meteorological Society* 83:1,631–1,643. (The updated data to 2005 were downloaded on March 22, 2005, from ftp://ftp.cdc.noaa.gov/Datasets/ncep.reanalysis2/gaussian.grid.)

Le Quéré, C., C. Rodembeck. E. Buitenhuis, T. Conway, R. Langenfelds, A. Gomez, C. Labuschagne, M. Ramonet, T. Nakazawa, N. Metzl, and others. 2007. Saturation of the Southern Ocean CO_2 sink due to recent climate change. *Science* 316:1,735–1,738, http://dx.doi.org/10.1126/science.1136188.

Le Quéré, C., T. Takahashi, E.T. Buitenhuis, C. Rodenbeck, and S.C. Sutherland. 2010. Impact of climate change and variability on the global oceanic sink of CO_2. *Global Biogeochemical Cycles* 24, GB4007, http://dx.doi.org/10.1029/2009GB003599.

Lenton, A., and R.J. Matear. 2007. Role of the Southern Annular Mode (SAM) in Southern Ocean CO_2 uptake. *Global Biogeochemical Cycles* 21, GB2016, http://dx.doi.org/10.1029/2006GB002714.

Lizotte, M.P. 2001. The contributions of sea ice algae to Antarctic marine primary production. *American Zoologist* 41:57–71, http://dx.doi.org/10.1093/icb/41.1.57.

Lovenduski, N.S., N. Gruber, S.C. Doney, and I.D. Lima. 2007. Enhanced CO_2 outgassing in the Southern Ocean from a positive phase of the Southern Annual Mode. *Global Biogeochemical Cycles* 21, GB2026, http://dx.doi.org/10.1029/2006GB002900.

Manning, A.C., and R.F. Keeling. 2006. Global oceanic and land biotic carbon sinks from the Scripps atmospheric oxygen flask sampling network. *Tellus* 58B:95–116, http://dx.doi.org/10.1111/j.1600-0889.2006.00175.x.

Metzl, N., C. Brunet, A. Jabaud-Jan, A. Poisson, and B. Schauer. 2006. Summer and winter air-sea CO_2 fluxes in the Southern Ocean. *Deep Sea Research Part I* 53:1,548–1,563, http://dx.doi.org/10.1016/j.dsr.2006.07.006.

Metzl, N. 2009. Decadal increase of oceanic carbon dioxide in Southern Indian Ocean surface waters (1991–2007). *Deep Sea Research Part II* 56:607–619, http://dx.doi.org/10.1016/j.dsr2.2008.12.007.

Mikaloff Fletcher, S.E., N. Gruber, A.R. Jacobson, S.C. Doney, S. Dutkiewicz, M. Gerber, M. Follows, F. Joos, K. Lindsay, D. Menemenlis, and others. 2006. Inverse estimates of anthropogenic CO_2 uptake, transport, and storage by the ocean. *Global Biogeochemical Cycles* 20, GB2002, http://dx.doi.org/10.1029/2005GB002530.

Moore, J.K., and M.R. Abbott. 2000. Phytoplankton chlorophyll distributions and primary production in the Southern Ocean. *Journal of Geophysical Research* 105:28,709-28,722, http://dx.doi.org/10.1029/1999JC000043.

NCEP/DOE 2 Reanalysis Data. 2005. Ice field data provided by NOAA/OAR/ESRL PSD, Boulder CO, via web site: http://www.esrl.noaa.gov/psd/data/gridded/data.ncep.reanalysis2.gaussian.html.

Newberger, T. 2004. Underway pCO_2 System Users Manual, Palmer 2004 pCO_2 System. Lamont-Doherty Earth Observatory, Palisades, NY, 23 pp., http://www.ldeo.columbia.edu/res/pi/CO2/carbondioxide/text/Palmer_PCO2_man_1_2.pdf.

Orsi, A.H., T. Whitworth III, and W.D. Nowlin. 1995. On the meridional extent and fronts of the Antarctic Circumpolar Current. *Deep Sea Research Part I* 42:641–673, http://dx.doi.org/10.1016/0967-0637(95)00021-W.

Quay, P., R. Sommerup, T. Westby, J. Sutsman, and A. McNichol. 2003. Changes in the $^{13}C/^{12}C$ of dissolved inorganic carbon in the ocean as a tracer of anthropogenic CO_2 uptake. *Global Biogeochemical Cycles* 17(1), 1004, http://dx.doi.org/10.1029/2001GB001817.

Rubin, S.I. 2003. Carbon and nutrient cycling in the upper water column across the Polar Frontal Zone and Antarctic Circumpolar Current along 170°W. *Global Biogeochemical Cycles* 17, 1087, http://dx.doi.org/10.1029/2002GB001900.

Rubin, S.I., T. Takahashi, D.W. Chipman, and J.G. Goddard. 1998. Primary production and nutrient utilization ratios in the Pacific Sector of the Southern Ocean based on seasonal changes in seawater chemistry. *Deep Sea Research* 45:1,211–1,234, http://dx.doi.org/10.1016/S0967-0637(98)00021-1.

Sabine, C.L., R.A. Feely, N. Gruber, R.M. Key, K. Lee, J.L. Bullister, R. Wanninkhof, C.S. Wong, D.W.R. Wallace, B. Tilbrook, and others. 2004. The oceanic sink for anthropogenic CO_2. *Science* 305:367–371, http://dx.doi.org/10.1126/science.1097403.

Sarmiento, J.L., and N. Gruber. 2006. *Ocean Biogeochemical Dynamics*. Princeton University Press, Princeton, NJ, 503 pp.

Signorini, S.R., and C.R. McClain. 2009. Effect of uncertainties in climatologic wind, ocean pCO_2, and gas transfer algorithms on the estimate of global sea-air CO_2 flux. *Global Biogeochemical Cycles* 23, GB2025, http://dx.doi.org/10.1029/2008GB003246.

Sweeney, C. 2003. The annual cycle of surface CO_2 and O_2 in the Ross Sea: A model for gas exchange on the continental shelves of Antarctica. Pp. 295–312 in *Biogeochemistry of the Ross Sea*. G.R. DiTullio and R.B. Dunbar, eds, Antarctic Research Series, vol. 78, American Geophysical Union, Washington, DC, http://dx.doi.org/10.1029/AR078.

Sweeney, C., E. Gloor, A.R. Jacobson, R.M. Key, G. McKinley, J.L. Sarmiento, and R. Wanninkhof. 2007. Constraining global air-sea gas exchange for CO_2 with recent bomb ^{14}C measurements. *Global Biogeochemical Cycles* 21, GB2015, http://dx.doi.org/10.1029/2006GB002784.

Takahashi, T., and D.W. Chipman. 2012. CO_2 transport in deep waters off Wilkes Land. *Oceanography* 25(3):24–25, http://dx.doi.org/10.5670/oceanog.2012.70.

Takahashi, T., S.C. Sutherland, R. Wanninkhof, C. Sweeney, R.A. Feely, D.W. Chipman, B. Hales, G. Friederich, F. Chavez, C. Sabine, and others. 2009. Climatological mean and decadal changes in surface ocean pCO_2, and net sea-air CO_2 flux over the global oceans. *Deep Sea Research Part II* 56: 554–577, http://dx.doi.org/10.1016/j.dsr2.2008.12.009.

Takahashi, T., S.C. Sutherland, and A. Kozyr. 2011. *Global Ocean Surface Water Partial Pressure of CO_2 Database: Measurements Performed During 1957–2010 (Version 2010)*. ORNL/CDIAC-159, NDP-088(V2010). Carbon Dioxide Information Analysis Center, Oak Ridge National Laboratory, U.S. Department of Energy, Oak Ridge, Tennessee, http://dx.doi.org/10.3334/CDIAC/otg.ndp088(V2010).

Wanninkhof, R. 1992. Relationship between wind speed and gas exchange. *Journal of Geophysical Research* 97:7,373–7,382, http://dx.doi.org/10.1029/92JC00188.

Weiss, R.F. 1974. Carbon dioxide in water and seawater: The solubility of a non-ideal gas. *Marine Chemistry* 2:203–215, http://dx.doi.org/10.1016/0304-4203(74)90015-2.

Worby, A.P., C.A. Geiger, M.J. Paget, M.L. Van Woert, S.F. Ackley, and T.L. DeLiberty. 2008. Thickness distribution of Antarctic sea ice. *Journal of Geophysical Research* 113, C05S92, http://dx.doi.org/10.1029/2007JC004254.